

SWNT-array resonant gate MOS transistor

A. Arun¹, S. Campidelli², A. Filoramo², V. Derycke², P. Salet¹,
A. M. Ionescu¹ and M. F. Goffman²

¹NanoLab, Ecole Polytechnique Fédérale de Lausanne, CH-1015, Lausanne,
Switzerland

²Laboratoire d'Electronique Moléculaire, SPEC (CNRS URA 2454), IRAMIS, CEA,
Gif-sur-Yvette, France

E-mail: marcelo.goffman@cea.fr

Abstract. We show that thin horizontal arrays of single wall carbon nanotubes (SWNTs) suspended above the channel of silicon MOSFETs can be used as vibrating gate electrodes. This new class of nano-electromechanical system (NEMS) combines the unique mechanical and electronic properties of SWNTs with an integrated silicon-based motion detection. Its electrical response exhibits a clear signature of the mechanical resonance of SWNTs arrays (120-150 MHz) showing that these thin horizontal arrays behave as a cohesive, rigid and elastic body membrane with a Young modulus in the order of 1-10 GPa and ultra-low mass. The resonant frequency can be tuned by the gate voltage and its dependence is well understood within the continuum mechanics framework.

PACS numbers: 62.25.-g 68.35.Gy 81.07.-b 81.07.Oj 81.16.Dn 85.35.Kt 85.85.+j

It is largely admitted that the future integration of nano-objects within technologically relevant devices and circuits will require their co-integration with the existing CMOS technology. Yet, examples of functional devices and circuits combining the two types of building blocks are extremely scarce. Among the different nano-objects, carbon nanotubes (CNTs) have attracted much attention due to their unique electronic properties. Examples of integration of CNTs with CMOS-based electronic circuits are limited to field effect transistors (FET) [1] and interconnects [2]. Moreover, since CNTs are light and have very large Young's modulus [3] they constitute an ideal building block for devices such as micro and nano-electromechanical systems (MEMS/NEMS). Most of the efforts to date have primarily focused on individual CNT based nanodevices. For example, a suspended nanotube has been used as a device element of a tuneable electromechanical oscillator [4, 5], sensors [6, 7], rotational actuators [8]. Similarly, a carbon nanotube cantilever has been used in scanning probe microscope tips [9], nanotweezers [10], switches [11, 12] and relays [13] and even a nanotube radio [14]. These demonstrations mainly require dedicated nanofabrication steps for aligning the measuring circuit to the position of individual CNTs and/or tedious and time consuming manipulation of CNTs, making the realization of reliable and integrated nanodevices impractical. Recently an elegant approach was demonstrated to circumvent this problem, by synthesizing three-dimensional CNT medium composed mostly of highly-oriented and closely packed CNTs [15]. Using this approach, thick "CNT wafers" can be deposited on top of a prefabricated silicon wafer and post-processed, paving the way to the integration of hybrid CNT-silicon devices. In order to assess the potential of "CNT wafers" as micromechanical material, Hayamizu *et al.* [16] investigated the mechanical properties of thick beams and found that they act as a single cohesive unit described by classical theory of elasticity. On the opposite limit, thin SWNTs arrays used in SWNT-based field effect transistors showed very promising high frequency electronic properties [17]. If in addition these extremely thin SWNT layers show interesting mechanical properties they could serve as a basic material for innovative MEMS/NEMS devices. Of particular interest are movable gate [18, 19] and body FET transistor structures [20, 21] operating as active MEM/NEM resonators, similarly to the very first proposed resonant-Gate transistor [22].

Here we present an alternative way, versatile and well adapted to integrate extremely thin SWNTs arrays to CMOS transistors and demonstrate the first resonant SWNTs array suspended gate FET, fully compatible with any bulk silicon CMOS technology. The SWNTs suspended gate FET device (SWNTs SG-SiFET) combines the virtues of SWNT suspended arrays (stiff and light material used as vibrating gate of a silicon field effect transistor (SiFET)), with the integrated transistor detection. The high frequency vibration of the SWNTs array modulates the charge density in the FET channel and the output signal of the resonator is the drain current. The electrical response shows the signature of the mechanical resonance of SWNTs arrays (120-150 MHz) demonstrating that these extremely thin horizontal arrays behave as a cohesive, rigid and elastic body membrane. The resonant frequency can be tuned by the gate voltage and its dependence

is well understood within the continuum mechanics framework.

Figure 1 shows a micrograph of a SWNTs SG-SiFET and its schematic cross section. The fabrication details of the SiFET are described elsewhere [23]. Suspended SWNTs gates centered on the FET channel were fabricated as follows: First, chromium/platinum Cr/Pt (5 nm/ 60 nm) lines were patterned perpendicular to the FET channel (See 1 A and B). These electrodes were used to deposit a dense array of SWNTs, mostly centered on top of the SiFET channel, by a dielectrophoresis (DEP) process. The DEP step is described in detail elsewhere [17]. The SWNTs used were synthesized by laser ablation, first purified and then dispersed at low concentration in *N*-methylpyrrolidone using moderate sonication, resulting in a highly stable dispersion comprising mostly individual nanotubes. To give a precise geometry to the SWNTs gate, an e-beam lithography step followed by reactive ion etching (O_2/SF_6) was realized. Finally Ti/Au (10 nm/ 50 nm) electrodes were patterned by e-beam lithography and lift-off technique to doubly clamp and electrically contact the SWNTs gate to metallic lines. The SWNTs gate was suspended by etching the sacrificial layer in BHF. This step was done only in the central region, through an e-beam patterned PMMA mask, to avoid damaging of Al electrodes of the SiFET. The e-beam mask was stripped in acetone followed by critical point drying. The final air-gap of the fabricated device is 100nm, with a residual oxide thickness of 35 nm.

The SWNTs array gate is actuated by applying a V_G voltage on the suspended SWNTs membrane gate. The electrostatic force on the SWNTs membrane for $V_G = V_G^{DC} + v_G \cos \omega t$ and $V_G^{DC} \gg v_G$ can be well approximated by

$$F_{el} \simeq \frac{1}{2} C'_G V_G^{DC*} [V_G^{DC*} + 2v_G \cos \omega t] \quad (1)$$

where C'_G is the first derivative of the gate capacitance per unit length with respect to the gap separation and $V_G^{DC*} = V_G^{DC} - V_{Gint}$ and V_{Gint} the mean value of the channel potential [24]. The first term of (1) corresponds to the DC component that elastically deforms the SWNTs membrane and sets its mechanical tension and the second drives its motion at frequency ω . The SWNTs membrane motion induced by the AC component of F_{el} modulates the capacitance δC_G which in turn modulates the charge in the channel. The conductance channel change δG can be written as

$$\delta G \simeq \frac{dG}{dV_G} \left(v_G \cos(\omega t) + \frac{\delta C_G}{C_G}(\omega) \cdot V_G^{DC*} \right) \quad (2)$$

To detect this conductance change at ω we use the device as a mixer: we apply an AC voltage $v_{DS} \cdot \cos(\omega t - \varphi)$ between source and drain [25] and an AC gate voltage $v_G \cdot \cos(\omega t)$ chopped by a switch operated at audio frequency f_A (typically 133 Hz, see setup depicted in Figure 2).

The source-drain current has a component I^{LI} at f_A which is detected by a lock-in amplifier:

$$I^{LI} = \frac{\sqrt{2}}{\pi} \frac{dG}{dV_G} \left(\frac{\delta C_G}{C_G} V_G^{DC*} + v_G \right) \cdot v_{DS} \quad (3)$$

The first term contains the mechanical response of the SWNTs array. For small motional amplitudes, the membrane can be treated as a simple harmonic resonator [26] with effective mass $M = \xi\rho WLH$, $\xi \cong 1.44858$ and ρ , W , L and H are the mass density, width, length and thickness of the membrane respectively. The change in capacitance $\delta C_G(\omega)$ can be well approximated by $\delta C_G(\omega) \cong \tilde{C}'_G \cdot \delta y(\omega)$ where $\delta y(\omega)$ is the displacement of the midpoint of the resonator and can be obtained from the effective harmonic oscillator equation (see Equation (6) below):

$$\delta y(\omega) = \frac{\tilde{C}'_G V_G^{DC*} v_G}{M} [\text{Re}Y(\omega) \cos \omega t - \text{Im}Y(\omega) \sin \omega t] \quad (4)$$

Where $Y = (\omega_0^2 - \omega^2 + j\omega_0\omega/Q)^{-1}$ is the response function of a harmonic oscillator with resonant frequency ω_0 and quality factor Q , driven at frequency ω . Then the lock-in current reads:

$$I^{LI} = I_B (A (\text{Re}Y \cdot \cos \varphi + \text{Im}Y \cdot \sin \varphi) + \cos \varphi) \quad (5)$$

Where $I_B = \sqrt{2}/\pi (dG/dV_G) v_{DS} v_G$, $A = \frac{(\tilde{C}'_G)^2}{M\tilde{C}_G} (V_G^{DC} - V_{Gint})^2$ and the phase difference between the RF signal on the gate and source electrodes is φ . Using this expression, data can be fitted and the gate voltage dependence of the resonant frequency $f_0 (V_G^{DC}) = \omega_0/2\pi$ and the quality factor Q can be estimated.

Figure 3 shows the mixing current I^{LI} measured on device #1 ($L = 800 \text{ nm}$) as a function of the excitation frequency for 5 different values of V_G^{DC} and their best fit using expression (5) and I_B , A , ω_0 , Q and φ as fitting parameters. Data were taken in the linear regime (low AC amplitudes) under vacuum (10^{-5} mbar) and at room temperature. The size of the resonance feature increases with increasing the DC gate voltage making evident the increase of the SWNTs membrane deflection amplitude. The position in frequency of the resonance (in the 150-160 MHz range) moves downward with the increase of the gate voltage showing an counter-intuitive effective softening of the SWNTs membrane spring constant. Thanks to the array configuration, the output signal level of our SWNTs array resonator is approximately one order of magnitude higher than the one reported in Ref.[4] and [28], using a mixing configuration scheme, which highlights the advantages of a hybrid SWNTs/SiFET configuration for building MEM oscillators. Moreover, the output signal level of the SWNTs array SG-SiFET can be further increased by operating the transistor at higher DC V_{DS} (saturation mode). In this work, we mainly focus on the electromechanical behavior of the SWNTs array and in demonstrating the basic operating behavior of such device.

Figure 4 shows the extracted resonant frequency for two different devices: #1 and #2 ($L = 800\text{nm}$ and 1000nm respectively). As expected, the resonant frequency extrapolated to zero gate voltage is higher for device #1 since the array length is smaller. For device #2 we observe a decrease at low gate voltages and a strong increase at higher voltages.

To explain the observed dependence, we consider the SWNTs array as an effective beam [27] and we use a continuum model to describe its electromechanical behavior. Such approach was successfully used in the case of individual MWNTs in Ref.[28]. If we assume that the driving electrostatic force does not change the shape of lowest vibration mode of the SWNTs array $u_1(x)$, the vertical displacement of the SWNTs array $y(x, t)$ can be approximated by $y_0(x) + u_1(x) \cdot \delta y(t)$, i.e. a stationary part obeying the beam equation determined by the DC electrostatic force and a small time dependent part $\delta y(t)$ obeying the equivalent harmonic oscillator equation (see Supplementary Information (SI) for details)

$$M \frac{d^2 \delta y}{dt^2} + \mu \frac{d \delta y}{dt} + K \cdot \delta y = \tilde{C}'_G V_G^{DC*} v_G \cdot \cos(\omega t) + \tilde{C}''_G (V_G^{DC*})^2 \cdot \delta y \quad (6)$$

in (6) the spring constant K is determined by the physical and geometrical parameters of the SWNTs array and the mechanical tension set by V_G^{DC} . As can be expected, the spring constant K is an increasing function of V_G^{DC} since the mechanical tension increases with V_G^{DC} . The value of K can be obtained by solving self-consistently the beam equation (see SI for details). The second term on the right-hand side of (6) comes from the non-linear dependence of the gate capacitance C_G with the vertical coordinate. This term renormalizes the spring constant and produces a softening of the resonator. Then the resonant frequency of the SWNTs array can be written as follows (see SI for details)

$$f_0(V_G^{DC}) = \frac{1}{2\pi} \sqrt{\frac{K - \tilde{C}''_G (V_G^{DC*})^2}{M}} = \sqrt{f_1^2 \left(1 + \alpha \tilde{T}_0\right) - \beta \cdot (V_G^{DC*})^2 + f_1^2 \alpha \int_0^1 \left(\frac{dy_0}{dx}\right)^2 dx + f_1^2 \kappa \left(\int_0^1 \frac{d^2 y_0}{dx^2} u_1(x) dx\right)^2} \quad (7)$$

where $f_1 \simeq 1.03 \frac{H}{L^2} \sqrt{E/\rho}$ corresponds to the fundamental resonant frequency of a doubly clamped beam, $\alpha \simeq 0.1475$, $T_0 = \tilde{T}_0 (EWH^3/2L^2)$ is the mechanical residual tension when $V_G^{DC*} = 0$, $\beta = \varepsilon_0/(4\pi^2 \rho H \cdot H_0^3)$ and $\kappa \simeq 0.0166$. The third and fourth terms in (7) are the DC gate voltage dependent hardening of the effective spring constant due to the elastic deformation of the beam. Numerical simulations show that the sum of these two terms can be written as $\lambda(E, \tilde{T}_0) \cdot (V_G^{DC*})^4$. As a result, the proposed model fits quantitatively our data if $\beta \gg \lambda(E, \tilde{T}_0)$.

AFM characterization of our devices shows that the thickness of the SWNTs array is inhomogeneous. The mean value of the SWNTs membrane thickness is about (20 ± 10) nm for both devices. The imperfect packing and alignment of SWNTs, that produces the mechanical cohesiveness of the SWNTs membrane, makes its density unknown. However, from data at low gate voltages one could estimate the value of β and use its definition to obtain an effective density ρ_{eff} . This yields: (700 ± 400) Kg \cdot m $^{-3}$ for

device #1 and $(400 \pm 200) \text{ Kg} \cdot \text{m}^{-3}$ for device #2. Using this estimation and E and T_0 as fitting parameters one could obtain the results depicted in Figure 4. For comparison we also show the best result considering $T_0 = 0$ (black dash curve) and using only E as fitting parameter (120 GPa and 610 GPa for device #1 and #2 respectively). The red curves correspond to the best fit: $E = (3 \pm 1.5) \text{ GPa}$, $T_0 = (2 \pm 0.1) \mu\text{N}$ for device #1 and $E = (10 \pm 5) \text{ GPa}$, $T_0 = (1 \pm 0.1) \mu\text{N}$ for device #2. Gray region represents the uncertainty on the thickness H for device #1 and the sensitivity to the value of E for device #2. The quantitative agreement makes evident the finite value of an in-built mechanical tension. This mechanical tension can probably be attributed to the suspension step of SWNTs membranes. The impact of dielectrophoresis field on T_0 will be further investigated. The value obtained for the Young's modulus is better than the one reported for bucky paper [30] 2.3 GPa and comparable to the one reported for highly aligned SWNTs [15] or slightly smaller [16], supporting that our SWNTs arrays of thickness as small as 15nm behaves as highly ordered wafers.

The quality factor obtained from fitting $I^{LI}(\omega)$ is 35 – 55 for both devices. This value is comparable to the one reported by Hayamizu *et al.* [16] for highly aligned SWNTs thick cantilevers ($H \cong 250\text{nm}$) and suspended graphene [31] but lower than the one reported for single arc discharged SWNTs [9]. One possible explanation is related to the energy loss due to loosely linked SWNTs inside the membrane. This value could be improved by suppressing the sliding among SWNTs via cross-linking between them, as suggested in [32].

In conclusion, SWNT suspended membrane gates were successfully integrated to MOS transistors and operated at high frequency for the first time. These extremely thin membranes behave as a cohesive, rigid and elastic body. In particular, the resonant frequency of SWNTs SG-SiFETs is tuned by the DC gate voltage and its dependence can be well described within the continuum mechanics framework. The mechanical properties of SWNTs arrays are comparable to those observed in closely packed and aligned SWNTs wafers [15]. The quality factor observed makes SWNTs membranes more suitable for high frequency mechanical switching devices because of the quick damping of vibration. This work shows promise to realize devices with practical application using CNT, for example in bio-sensing and RF electronics.

Acknowledgments

This work was supported by Nano-RF, FP6 European project. We thank P. Joyez and C. Urbina for critical reading of the manuscript.

- [1] Tseng Y 2004 *et al. Nano Lett.*, **4** 123
- [2] Close G F 2008 *et al. Nano Lett.***8** 706
- [3] Treacy M M J, Ebbesen T W, Gibson J M 1996 *Nature* **381** 678.
- [4] Sazonova V *et al.*2004 *Nature* **431** 284
- [5] Witkamp B, Poot M and van der Zant H S J 2006 *Nano Lett.* **12** 2904
- [6] Kong J *et al.* 2000 *Science* **287** 622
- [7] Stampfer, *et al.* 2006 *Nano Lett.* **6** 233
- [8] Fennimore A M, *et al.* 2003 *Nature* **424** 408
- [9] Dai H *et al.* 1996 *Nature* **384** 147
- [10] Kim P and Lieber C M 1999 *Science* **286** 2148
- [11] Dujardin E, *et al.* 2005 *Appl. Phys. Lett.* **87** 193107
- [12] Jang J E , *et al.* 2008 *Nat. Nanotechnol.* **3** 26
- [13] Lee S W *et al.* 2004 *Nano Lett.* **4** 2027
- [14] Jensen K, Weldon J, Garcia H and Zettl A 2007 *Nano Lett.* **7** 3508
- [15] Hayamizu Y. *et al.* 2008 *Nat. Nanotechnol.* **3** 289
- [16] Hayamizu Y *et al.* 2009 *Phys. Rev. Lett.* **102** 175505.
- [17] Le Louarn A *et al.* 2007 *Appl. Phys. Lett.* **90** 233108
- [18] Abele N, *et al.* 2005 *Technical IEEE International Digest Electron Devices Meeting, IEDM* **479** 1967
- [19] Durand C *et al.* 2008 *IEEE Electron Device Letters* **29** 494
- [20] Grogg D, *et al.* 2008 *Digest of Annual Device Research Conference, DRC 2008* 155
- [21] Grogg D, *et al.* 2008 *IEEE International Electron Devices Meeting, IEDM 2008* 1.
- [22] Nathanson H C, *et al.* 1967 *IEEE Transactions on Electron Devices, ED-14(3)* 117
- [23] Arun A *et al.* 2010 *IEEE proceedings of MEMS 2010* 112
- [24] SI describes the procedure used to estimate its value.
- [25] The phase difference between the gate and source electrode depends on the frequency of the rf signals, on the (gate dependent) conductance of the nanotube, and on its derivative. Moreover, the lock-in detected phase does not contain any information about φ .
- [26] Yurke B *et al.* 1995 *Phys. Rev. A* **51** 4211
- [27] As a first approximation we consider the membrane as a beam neglecting the correction due to the Poisson's ratio. This is justified by the small value generally observed for the shear modulus in this material.
- [28] Lefevre R, *et al.* 2005 *Phys. Rev. Lett.* **95** 185504
- [29] Saito R Dresselhaus G and Dresselhaus M S 1998 *Physical Properties of Carbon Nanotubes* (London: Imperial College Press)
- [30] Coleman J N *et al.* 2003 *Appl. Phys. Lett.* **82** 1682
- [31] Scott Bunch J, *et al.* 2007 *Science* **315** 490; Chen C, *et al.* 2009 *Nat. Nanotechnol.* **4** 861
- [32] Kis A, *et al.* 2004 *Nat. Mater.* **3** 153

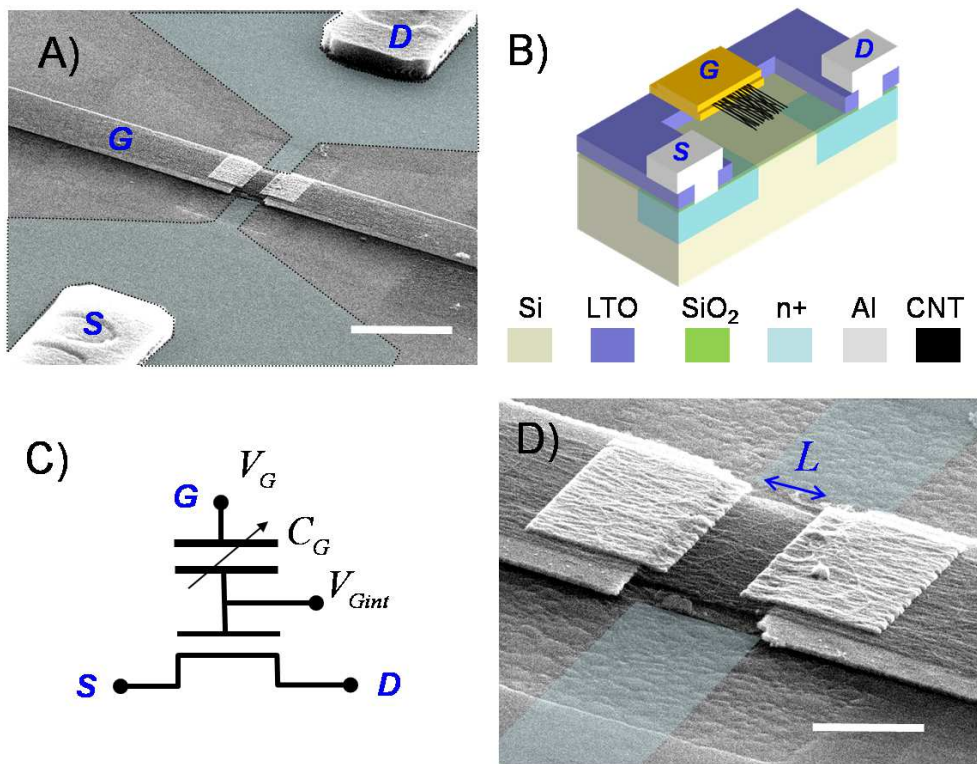


Figure 1. A) Micrograph of a SWNTs SG-SiFET. Scale bar: $5\mu\text{m}$. Light blue: ion implanted regions. B) Schematic cross section of a SWNTs SG-SiFET device: Si: silicon wafer (p-type; resistivity: 0.1 - 0.5 Ohm cm). LTO: low temperature silicon dioxide deposited to reduce the parasitic capacitance component from the substrate. n+: ion implanted regions to form source(S) and drain(D) contacts. Al: S and G contacted with aluminium Al lines are 50-Ohm designed. CNT: SWNT array deposited by DEP (see details in the text). C) Electrical circuit of a SWNTs SG-FET. C_G is the SWNTs gate capacitance per unit length. The SWNTs gate forms a thin SWNTs membrane on top of the FET channel which can be actuated by applying a voltage difference between the gate and the channel. D) Detailed view of the SWNTs array. Scale bar: $1\mu\text{m}$.

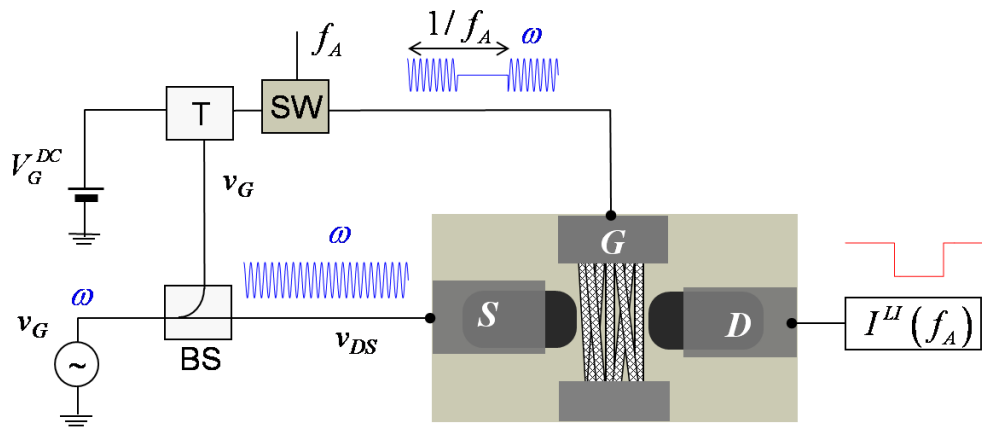


Figure 2. Diagram of the measurement setup. BS: beam splitter. SW: GaAs TTL switch. The device is operated as a mixer. A single rf generator provides two AC voltage signals: one amplitude modulated by SW (operated at f_A) and applied to the gate electrode to drive the suspended nanotube array and a second applied to the S electrode (v_{DS}). A DC gate voltage is added via a bias-T (indicated by the “T”). Its role is twofold: modify the operating point of the FET and set the mechanical tension of the SWNTs array. At the drain electrode D, the mixing current has a spectral component at f_A which is measured with a lock-in amplifier.

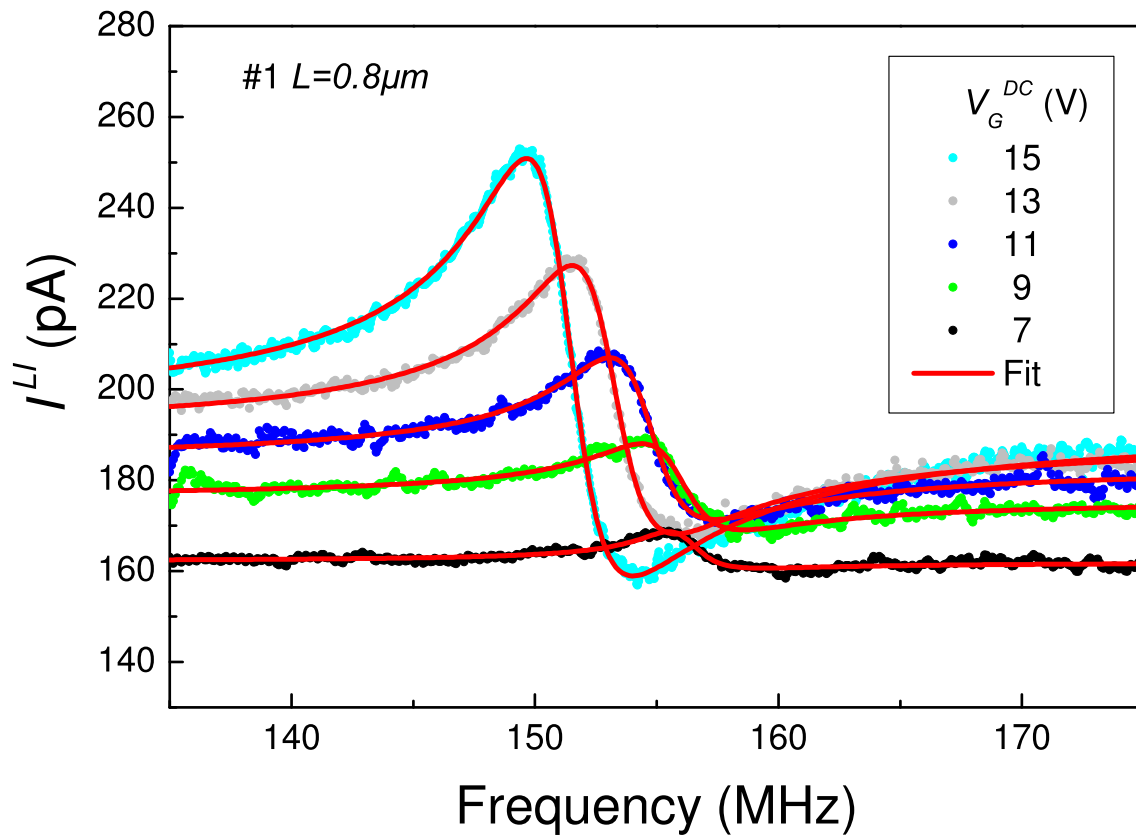


Figure 3. Mixing current I^{LI} as a function of the driving frequency for different values of V_G^{DC} for device #1. AC amplitudes are: $v_G = -29\text{dBm}$ and $v_{DS} = -24\text{dBm}$. Red curves: Best fit using Equation (5).

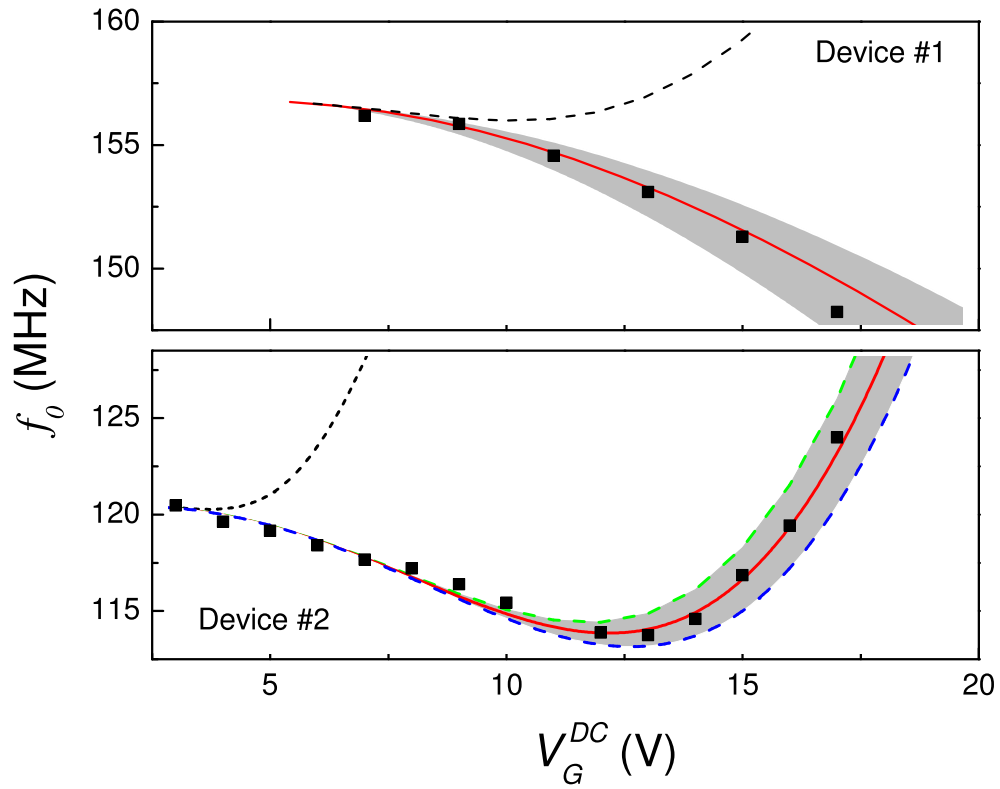


Figure 4. Resonant frequency as a function of V_G^{DC} extracted from the best fit of $I^{LI}(\omega)$ for device #1 (shown in 3) and device #2, $L = 800$ nm and 1000 nm respectively. Black dash curves: simulation using $T_0 = 0$. Red curves: best fits $E = (3 \pm 1.5)$ GPa $T_0 = (2 \pm 0.1) \mu\text{N}$ for device #1 $E = (10 \pm 5)$ GPa $T_0 = (1 \pm 0.1) \mu\text{N}$ for device #2. Gray regions represent the impact of thickness H uncertainty for device #1 and the sensitivity to the value of E for device #2. Dash green curve: $E = 11$ GPa $T_0 = 1 \mu\text{N}$. Dash blue curve: $E = 9$ GPa $T_0 = 1 \mu\text{N}$.